Rheol Acta (2010) 49:993–1001
DOI 10.1007/s00397-010-0466-5

ORIGINAL CONTRIBUTION

The effect of particle size and migration on the formation of flow-induced structures in viscoelastic suspensions

Rossana Pasquino · Frank Snijkers · Nino Grizzuti · Jan Vermant

Received: 2 January 2010 / Revised: 7 May 2010 / Accepted: 15 May 2010 / Published online: 8 June 2010

Abstract Flow-induced structures in suspensions containing spheres in viscoelastic suspending media were investigated by microscopy and rheo-optical methods. Suspensions of monodisperse polystyrene spheres with diameters ranging from 1.2 to 2.8 μm and dispersed in aqueous solutions of hydroxypropylcellulose were studied in simple shear flows. Optical microscopy observations as well as small-angle light-scattering (SALS) experiments were performed using a parallel plate geometry. In agreement with previous work, necklaces of particles aligned in the flow direction were observed when shearing faster then a critical shear rate, which was found to be independent of particle size. In contrast to earlier work, however, the role of particle migration was found to be of prime importance. Particles were shown to migrate toward the plates where the particles assembled and aligned in strings running in the flow direction. For the smallest particles (1 μm diameter), the formation of particle doublets or short strings along the vorticity direction was observed at low shear rates, which flipped to an orientation into the flow direction and grew into longer strings at higher shear rates. SALS experiments were used to quantify the degree of alignment and its dependence on particle size, shear rate, and gap. For the system under investigation, the degree of alignment was found to increase with increasing shear rate and particle size and with decreasing gap. The present results suggest that, depending on the details of the suspending medium and the size and nature of the suspended particles, the formation of aligned structures is affected by the relative magnitude of the colloidal and hydrodynamic forces and the kinetics of string formation versus the kinetics of migration.

Keywords Suspensions · Flow induced structures · Directed self-assembly · Particles in viscoelastic matrices

R. Pasquino (✉) · N. Grizzuti
Department of Chemical Engineering, University Federico II,
P. le Tecchio 80, 80125 Napoli, Italy
e-mail: rossana@iesl.forth.gr

F. Snijkers · J. Vermant
Department of Chemical Engineering,
Katholieke Universiteit Leuven,
Willem de Croylaan 46,
3001 Leuven, Belgium

J. Vermant
e-mail: jan.vermant@cit.kuleuven.be

Introduction

In many technological applications, particles are dispersed in fluids with a complex nonlinear rheological behavior, e.g., filled polymers, nanocomposites, paints, and some fancy consumer care products. The presence of the particles complicates the situation. Due to the changes in hydrodynamic interactions, the formation of strings or necklaces of particles in sheared viscoelastic fluids has been reported long ago. Michele et al. (1977) were the first to report results of string formation in what were described to be "monolayers" of semidilute suspensions of glass spheres in viscoelastic media, in the case of both oscillatory shear flow and pipe flow. Giesekus pointed out that this phenomenon was governed by the normal stress differences and furthermore showed that, in the case of a bidisperse suspension, the particles segregate and form separate strings, sorting themselves according to their size (Giesekus 1978,

1981). In earlier work, it was suggested that string formation only occurred above a critical Weissenberg number, Wi, defined here as the ratio of the first normal stress difference over the shear stress. However, more recently (Scirocco et al. 2004; Won and Kim 2004), it has been shown that the rheological effects of the suspending media are somewhat more subtle. No alignment could be observed in constant viscosity, highly elastic Boger fluids, whereas in weakly shear thinning Boger fluids, the critical Weissenberg number was found to be much larger than that observed for strongly shear thinning polymer solutions (Scirocco et al. 2004). In summary, the formation of particle strings parallel to flow direction is found to depend on a combination of shear thinning and fluid elasticity.

Most experimental investigations of flow-induced structure formation have relied on optical microscopy observations on thin samples, often not more than a monolayer of particles (Michele et al. 1977; Giesekus 1981; Lyon et al. 2001). It is not clear from these observations whether the alignment is wall-induced or is a bulk phenomenon. For one fluid/particle combination, i.e., 2.8 μm sized polystyrene spheres in a polymer solution with a viscous solvent, Scirocco et al. (2004) showed that there was virtually no dependence of the alignment on the gap size. However, for this specific fluid, no clear strings, rather bundles of particles were observed. Moreover, for the same particles in aqueous solutions of hydroxypropylcellulose (HPC), a deposition of the particles into crystalline patches onto the walls has been observed (Scirocco et al. 2004), suggesting that the strings—or the particles—undergo migration. Provided migration occurs, it can be expected to affect the alignment of particles into strings, as the gradients in concentration that are introduced by the migration will change the probability of particle interactions. Migration refers to the motion of particles from the bulk toward the confining walls. Like the factors controlling alignment, migration has been suggested to be promoted by normal stress differences and shear thinning (Jefri and Zahed 1989; Karnis and Mason 1966; Tehrani 1996). The role of normal stresses on particle migration was elucidated by theoretical calculations by Brunn (1976) and Ho and Leal (1976) and in simulations by Morris and Boulay (1999).

In the present work, the possible role of migration and wall effects on particle alignment are investigated by studying particles of monodisperse particles of different size in a aqueous solution of hydroxypropylcellulose. Suspensions are subjected to simple shear flow in a parallel plate geometry whose gap thickness is ten to hundred times larger than the particle size. Flow was generated in a rheo-optical shearing cell, and observations along the velocity gradient direction were made. The formation of flow-induced microstructures was followed qualitatively by optical video microscopy and quantitatively by small angle light scattering. In particular, the effects of shear rate, particle size, and gap thickness were studied.

Materials and methods

Monodisperse polystyrene (PS) spheres have been used as the dispersed phase. They were synthesized by a dispersion polymerization process, similar to the one described by Almog et al. (1982). The size of the resulting spheres is governed by the solubility of the polymer in the solvent with higher solubilities leading to larger particle sizes. The solubility of polystyrene was altered by changing the water content in the solvent. PS particles of 2.8, 1.9, and 1.2 μm (±0.1) diameter were synthesized. Particle density was reported to be about 1,050 kg/m^3, and the refractive index of PS is 1.59.

The suspending fluid was an aqueous solution of HPC (Klucel LF, Hercules) with a concentration of 30% by weight. The density of the suspending medium is about 1,100 kg/m^3, and the refractive index is 1.33. Sedimentation effects could be neglected on the time scale of experiments due to the high viscosity and small density mismatch between the particles and the fluid. Suspensions were prepared by hand mixing. For all experiments, a constant particle volume fraction of 0.8% was used. The calculated values of the particle Reynolds and Peclet numbers ($10^{-13} \leq Re_p \leq 10^{-10}$ and $10^4 \leq \mathrm{Pe} \leq 10^8$) ensured that inertia as well as Brownian forces can be neglected.

Rheo-optical experiments were performed using a parallel plate transparent flow cell (CSS 450, Linkam), which has been used for both optical microscopy and small-angle light-scattering (SALS) measurements. Observation were made along the velocity gradient direction, at a distance of 7.5 mm from the center of the parallel plate geometry. The viewing area was 2.5 mm in diameter. A transmitted light microscope was used (Leitz, Laborlux 12 POL-S) for bright field observations of the microstructure; images were captured by a 12-bit CCD camera (ORCA C4742-95, Hamamatsu).

In the SALS setup, a He/Ne laser beam was guided via a pinhole to the shearing cell. The scattered light was collected onto a semitransparent screen, and images were recorded by a CCD camera (Pulnix TM1300). The SALS time-resolved images were collected at preset time intervals by a digital frame

grabber and an in-house developed software (SALS SOFTWARE, KU Leuven). Rheological measurements on the unfilled suspending medium were carried out on a strain controlled rheometer (ARES, TA Instruments) equipped with a cone and plate geometry (plate diameter 25 mm, cone angle 0.1 rad). Temperature (20°C, as in the rheo-optical experiments) was controlled by means of Peltier elements, which guaranteed a thermal stability within ±0.1°C.

Results

Rheology

Cellulose solutions are notoriously difficult to deal with, in particular with respect to the heterogeneity of the solutions (Bodvik et al. 2010). To ensure a good dispersion of the cellulose, rheological experiments with different geometries were performed. The stability of the solution was checked by repeating the rheological measurements of the matrix fluids in time. The rheological response of the solutions remains unaltered when they are stored in the refrigerator for at least 2 weeks after the preparation. The rheological properties of the suspending medium are shown in Fig. 1. The zero rate shear viscosity is about 380 Pa s, and the suspension shear thins over two decades of shear rate. The Weissenberg number, Wi, defined as the ratio of the first normal stress difference over the shear stress, is also included in Fig. 1. The Weissenberg numbers as a function of shear rate can be well fitted by a power law:

$$\mathrm{Wi} = 0.48\dot{\gamma}^{0.50} \tag{1}$$

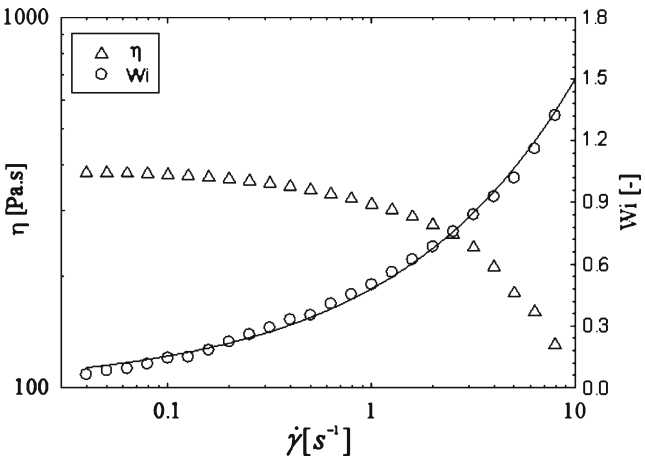

Fig. 1 Viscosity and Weissenberg number as a function of shear rate for the suspending medium

For the range of the shear rates studied, Wi never exceeds the value of 10.

Video microscopy during flow

In all rheo-optical experiments, a pristine sample was loaded in the Linkam, and the shear flow was started at time $t = 0$. A sample gap of 100 μm was always used in the microscopy experiments, unless noted otherwise. The evolution of the microstructure was observed as a function of time at different focusing depths. Shearing times as long as 1 h were applied. Figure 2 shows a typical time sequence for 2.8 μm sized particles for a system observed near the upper wall of the flow cell. At startup, a random particle distribution is present. After shearing for some time, an elongated, flow-oriented string-like structure develops. String length increases with shearing time until an essentially stationary microstructure is obtained.

The micrographs in Fig. 2 show that the particle number density increases with time, suggesting that string formation is accompanied by migration. To further clarify this point, we counted the spheres in focus directly from the microscopy images. The calculation is not highly precise but gives an idea of the increase of the amount of particles on the wall with time. There are about 200 particles in image a, 270 in image b, and 1,200 in image c; this corresponds to area fractions of 0.03, 0.04, and 0.17, respectively. The increase of particles at the wall in time is more directly confirmed in Fig. 3, where images near the wall and at the sample midplane are compared. After 1-h shearing, randomly distributed particles remain present in the bulk, whereas strings of particles are present near the wall (see Fig. 3a, b). It must be noticed that, for the systems studied here, alignment is not a bulk phenomenon. This result is in contrast with earlier literature reports and observations of similar PS particles in sheared PIB/PB solutions (Scirocco et al. 2004) and larger glass particles in polyacrylamide solutions (Michele et al. 1977).

Having established that particles migrate toward the wall and that alignment only occurs in its proximity, the effect of shear rate and particle size has been further investigated. Figure 4 shows the microstructure obtained after long times for a suspension of 1.9 μm beads, for different shear rates. Strings form only when a critical shear rate is exceeded. For the different sized particles, such a critical value falls within 1 and 5 s^{-1}. It should be noted that, at these shear rates, the Weissenberg number is smaller than 1 (Fig. 1) and that only weak shear thinning is present. This confirms that string formation readily occurs in weakly elastic, weakly shear thinning

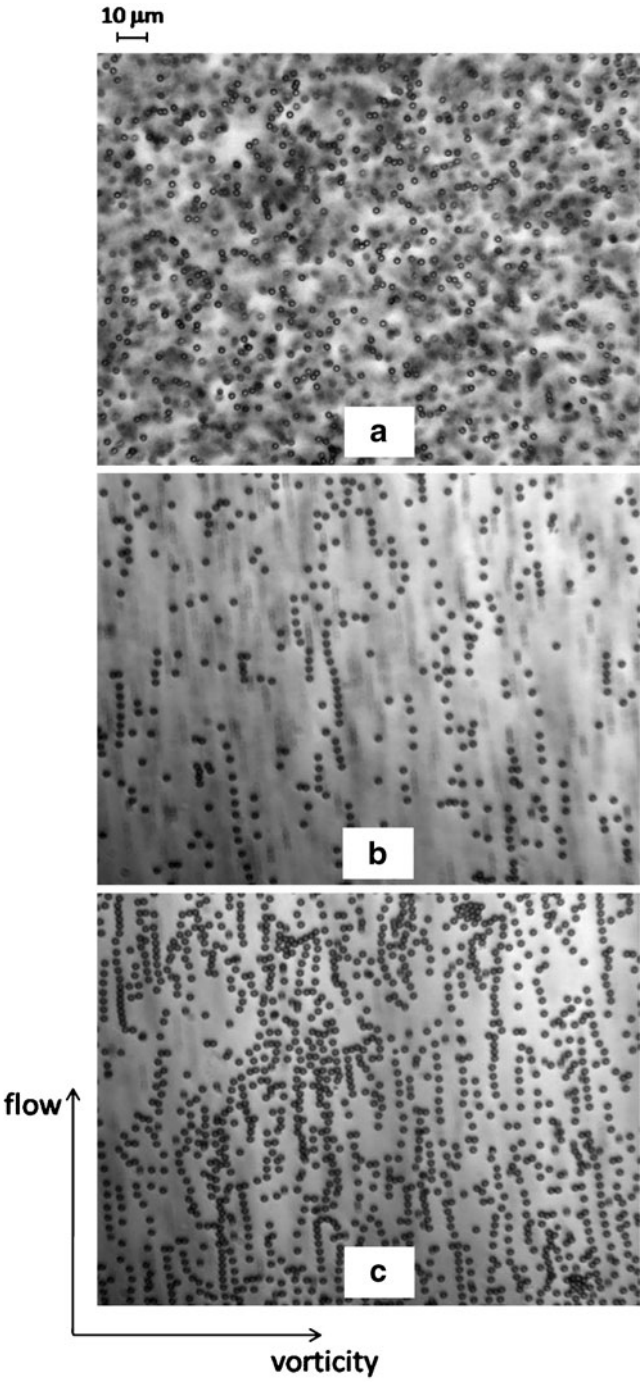

Fig. 2 Time evolution of the particle microstructure near the wall. **a** $t = 0$ s; **b** $t = 440$ s; **c** $t = 3{,}600$ s. Sphere size 2.8 μm. Shear rate 50 s^{-1}

fluids (Scirocco et al. 2004). At higher shear rates, the length of the strings increases, and they eventually regroup in bands which are separated by particle-free zones. An example is shown in Fig. 4e. This phenomenon has been previously observed in different flow geometries (Ponche and Dupuis 2005; Joseph and Feng 1996). The time required for string formation was found to be a decreasing function of the applied shear rate. A quantitative analysis of this aspect will be presented in the next section.

Changes in particle size to 1.9 μm did not produce substantial changes in the formation and evolution of the microstructure. A new phenomenon, however, was detected for the smallest spheres, i.e., 1.2 μm (see Fig. 5). These particles were observed to form doublets, triplet, or short strings that align in the vorticity rather than the flow direction at low shear rates (below about 1 s^{-1}). Vorticity alignment took place also in the bulk of the sample. This phenomenon, observed here for the first time, has no explanation at present. Low-shear rate alignment of ellipsoids along the vorticity axis has been already observed for viscoelastic fluids (Johnson and Fuller 1987; Gunes et al. 2008). In the present case, one can infer that, due to the small particle size (resulting in a higher surface area), short trains of particles may be stuck more strongly together by Van der Waals interactions or the adsorption of the HPC on the PS particles contributes to bridging flocculation, possibly enhance by flow. These elongated objects could be seen as equivalent to ellipsoids and thus behave in a similar fashion, as long as the hydrodynamic forces do not break them apart. The presence of the vorticity alignment, not perfectly clear from the microscopy observations, will be quantitatively demonstrated using SALS in the next section.

To summarize, in shear flow, in this rather weak shear thinning and mildly viscoelastic HPC solutions, micrometer-sized particles migrate toward the walls. Alignment in string-like structures in the flow direction takes place near or at the walls, only above a critical shear rate. The critical shear rate for the onset of alignment corresponds roughly to the beginning of the shear thinning region (between 1 and 5 s^{-1}). Beyond this critical rate, the degree of alignment increases with both time and rate, indicating that accumulated strain is a relevant parameter for this phenomenon. For sufficiently low shear rates and particles of sufficiently small-size, short vorticity-oriented particle chains could be observed.

Small angle light scattering

SALS experiments have been performed to provide a quantitative measure for the microstructures. Before discussing the results, it must be stressed that SALS patterns are an average over the whole sample thickness, whereas with optical microscopy, one can focus at different depths in the sample. In the SALS experiments, suspensions of various particle size were sheared

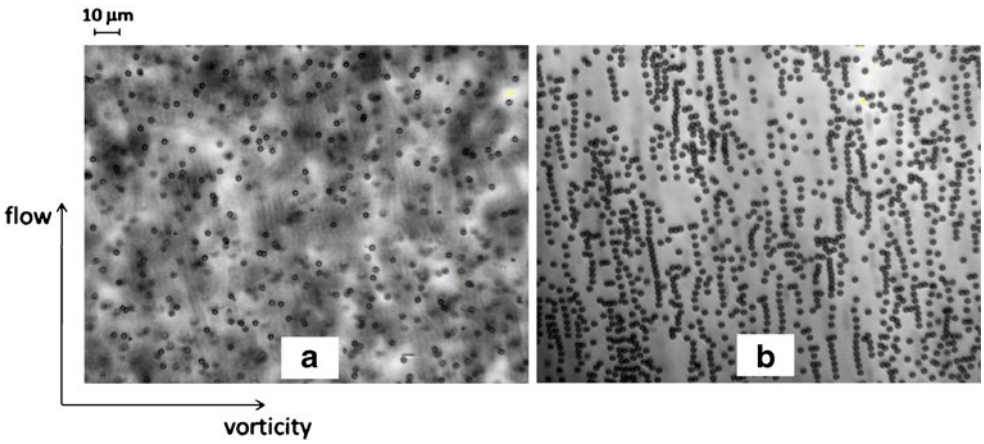

Fig. 3 Evolution of the suspension microstructure in the bulk and near the wall. **a** $t = 3{,}600$ s midplane; **b** $t = 3{,}600$ s wall. Sphere size 2.8 μm. Shear rate 30 s^{-1}

at different shear rates, and SALS patterns were recorded at fixed time intervals. Figure 6 shows the SALS patterns after 1 h time shearing at different shear rates for 1.2 μm size particles. At the lowest shear rate, the pattern is slightly elongated along the flow direction, indicating a weak alignment along the vorticity direction. As shear rate increases, a pronounced streak in the vorticity direction is observed, indicating alignment along the flow direction.

To quantitatively analyze the SALS patterns, the relative alignment factor is expanded in spherical harmonics, and the first term is integrated to get a measure for the degree of alignment. The relative alignment factor contains information about the form factor and the structure factor. In the analyzed q range, the form factor is nearly constant and equal to 1. The relative alignment factor can hence be considered a relative structure factor. Following Maranzano and Wagner (2002), a factor $\Delta A_f(q)$ is defined as:

$$\Delta A_f(q) = \int_0^{2\pi} [I(q,\theta)_{\dot{\gamma}} - I(q,\theta)_0] \cos(2\theta) d(\theta) \qquad (2)$$

where $I(q,\theta)$ is the scattering intensity at a given time and $I(q,\theta)_0$ is the one at startup. $\theta = 0$ is the flow direction. According to Eq. 2, this relative alignment factor is positive for a flow-oriented structure and negative for a vorticity-oriented structure. It is important to underline that we choose another type of definition for the alignment factor in comparison to the one from Scirocco et al. (2004) which is a normalized one. The factor $\Delta A_f(q)$ is more sensitive to compare flow induced changes.

The dependence of $\Delta A_f(q)$ on the scattering vector is in turn related to particle size. In order to correctly compare the results for different particle sizes, $\Delta A_f(q)$ was computed always at a specific value of the magnitude of the scattering vector, $q^*(1\ \mu m^{-1})$, such that $q^* \alpha R = \pi$, where R is the particle radius and α is a coefficient of order unity (a value $\alpha = 5$ was used). Furthermore, in order to minimize the experimental error due to scatter in the data, $\Delta A_f(q)$ was averaged over a range of scattering vectors $0.9q^* < q < 1.1q^*$.

Figure 7 compares the relative alignment factor after 1-h shearing (steady-state conditions) as a function of shear rate for different particle sizes. The alignment factor increases with increasing shear rate. For the two largest particle sizes, $\Delta A_f(q)$ is always positive, indicating that strings develop along the flow direction. For particles of 1.9 and 2.8 μm diameter, $\Delta A_f(q)$ was found to deviate from zero for shear rates between 1 and 5 s^{-1}, confirming the information obtained qualitatively from the optical microscopy. For the 1.2 μm size particles, negative values of $\Delta A_f(q)$ are measured at low shear rates, indicating the presence of ordered structures along the vorticity direction. Also, this result quantitatively confirms the observations presented in the previous section.

The alignment factor has also been studied as a function of sample thickness. Figure 8 shows the alignment factor at long times as a function of gap thickness for the 1.9 μm particles for different shear rates. As expected, $\Delta A_f(q)$ is a decreasing function of gap thickness, demonstrating that, for the present system, wall confinement is a key factor in the aligned flow-induced structures. At a given shear rate, larger values of ΔA_f are obtained for smaller gaps, indicating that alignment is enhanced by stronger confinement. When the gap becomes much larger than the sphere diameter (gap-particle ratio ~ 200), flow-induced microstructures are absent or, at least, its kinetics become extremely slow.

Some limited experiments have been performed to study the kinetics of flow-induced alignment. Figure 9 shows the time evolution of ΔA_f for the 1.9 μm particles at a shear rate of 30 s^{-1} for different gap sizes.

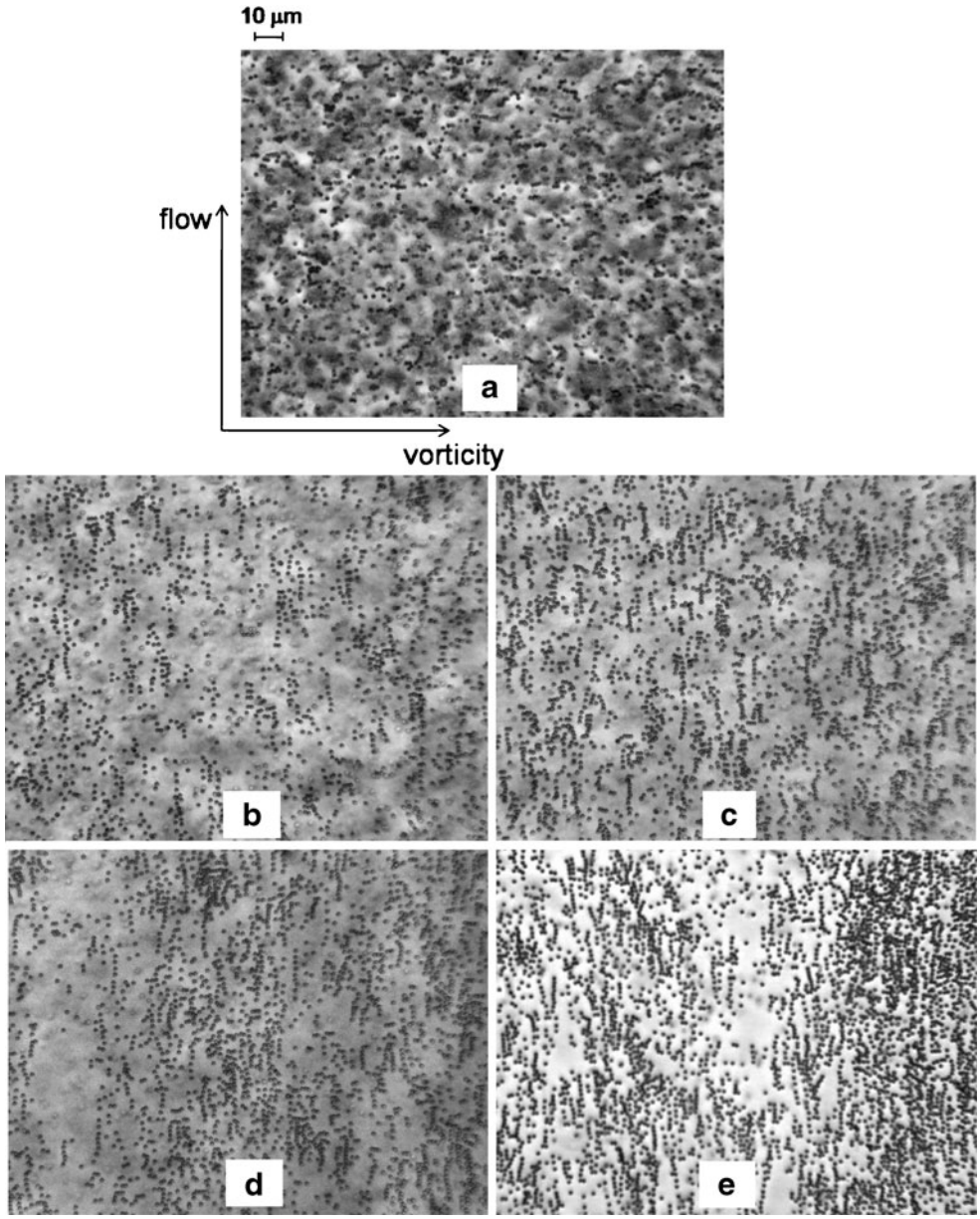

Fig. 4 Long-time microstructure at the wall for different shear rates: **a** 1 s^{-1}, **b** 5 s^{-1}, **c** 10 s^{-1}, **d** 30 s^{-1}, **e** 50 s^{-1}. Sphere diameter is 1.9 μm

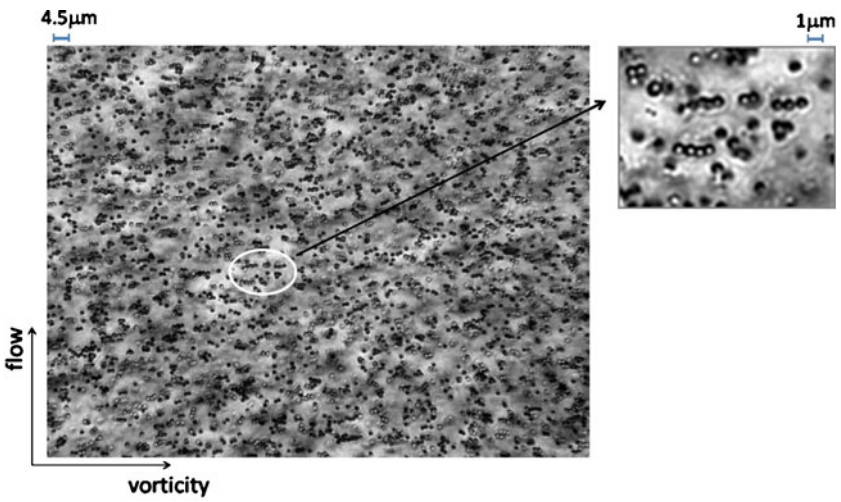

Fig. 5 Long-time microstructure in the bulk. Sphere diameter is 1.2 μm; shear rate = 1 s^{-1}. A weak vorticity-oriented structure can be detected

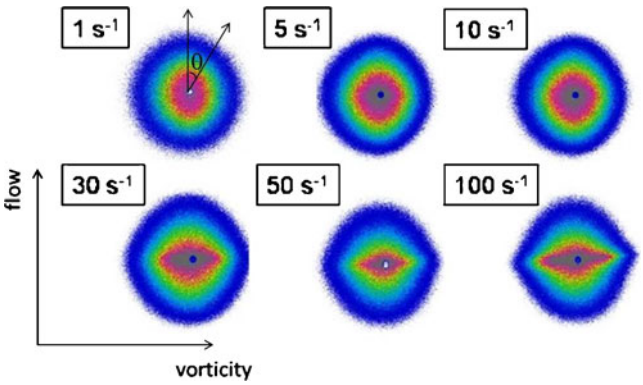

Fig. 6 SALS patterns as function of shear rate for 1.2 μm size particles. At low shear rates, a weak vorticity alignment of the real space structure can be seen

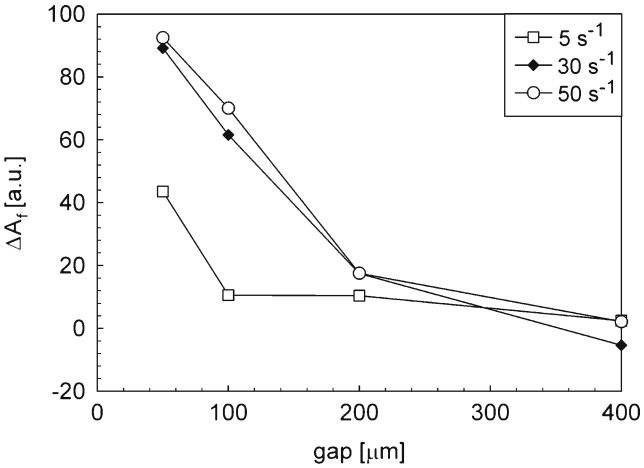

Fig. 8 The alignment factor after 1-h shearing as function of gap width for different shear rates. Particle size 1.9 μm

Steady-state conditions are reached at different times, depending on gap thickness. In particular, alignment occurs faster for smaller gaps and, as already shown in Fig. 8, smaller gaps result in higher alignment factor.

The results of Fig. 9 and the microscopy observations presented in the previous section suggest that particle migration and alignment are strongly coupled phenomena. It can be reasonably assumed that the smaller the gap size, the shorter the time necessary for particles to reach to wall, where alignment takes place. For the present suspending medium, which is only weakly shear thinning and only weakly elastic, the early stages of microstructure evolution are controlled by particle migration rather than particle alignment. This particle migration increases the concentration near the walls, which in turn leads to an increased probability of particles interacting. As a consequence, it can be argued that

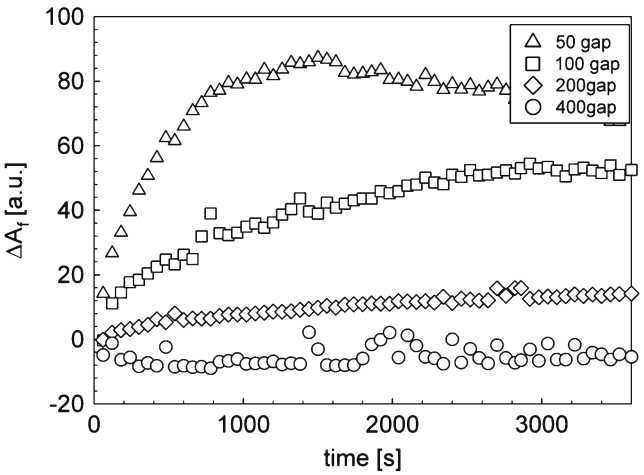

Fig. 9 Alignment factor as function of the time for different gap sizes. Particle size 1.9 μm. Shear rate 30 s^{-1}

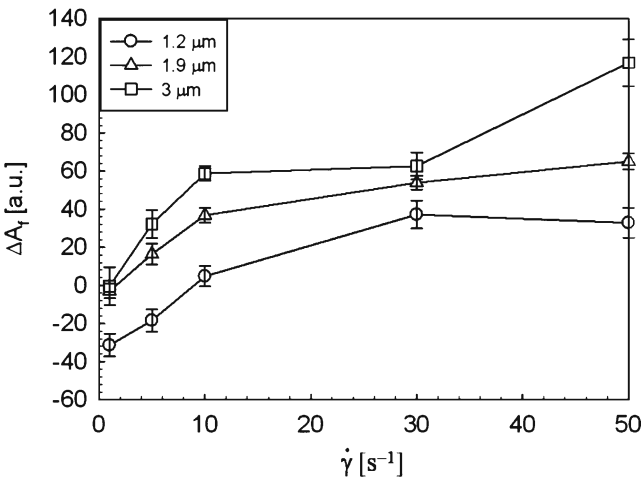

Fig. 7 The alignment factor after 1-h shearing as function of shear rate for suspensions of spheres with different sizes (gap = 100 μm)

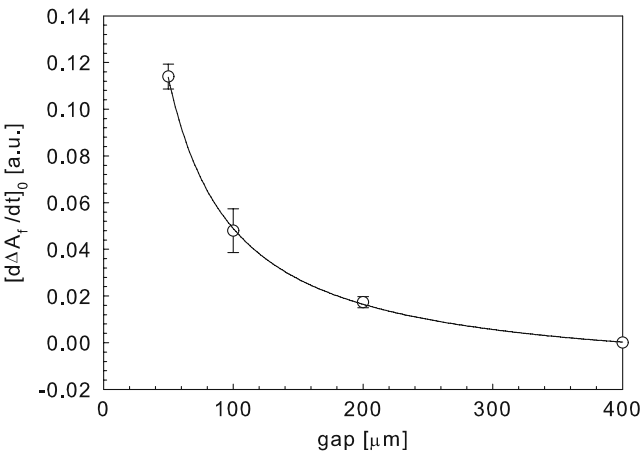

Fig. 10 The derivative of the alignment factor at flow startup as function of gap thickness. Particle size and shear rate as in Fig. 9. The *line* is the best fit to data

the initial rate of change of the alignment is a signature of the migration phenomenon. Figure 10 shows the derivative of the alignment factor upon startup of flow, $[d\Delta A_f/dt]_0$, as a function of gap thickness. $[d\Delta A_f/dt]_0$ is a strongly nonlinear function of gap thickness.

The effect of gap thickness on the alignment phenomena may well depend on the details of the rheology of the suspending medium. Migration is primarily controlled by the normal stress differences (Karnis and Mason 1966; Ho and Leal 1976; Lormand and Philips 2004), whereas the string formation and its kinetics depend also on the balance between the elastic forces, dependent on N_1 and the viscous forces that develop when two particles approach each other. The latter are determined by the overall level of the viscosity and the degree of shear thinning. For the suspending medium used here, the kinetics of migration are clearly faster than those of string formation. As the migration and string formation kinetics are determined by different rheological parameters, whether alignment occurs in the bulk (as in Michele et al. 1977; Scirocco et al. 2004) or near the walls (as in the case here), this will probably depend on the rheological properties of the suspending media.

Conclusions

When submitted to shear flow in confined geometries, suspensions in a weakly viscoelastic, shear thinning fluid showed a well-defined microstructure evolution, consisting of two parallel phenomena, namely migration from the bulk to the walls and formation of elongated strings in the flow direction at the wall. Microscopy observations showed that alignment is not generally a bulk phenomenon, as alignment took place only after migration of the major part of the particles toward the plates. The relative alignment factor measured with SALS experiments enabled a quantification of the alignment as a function of particle size, shear rate, and sample thickness. The measurements clearly indicated that alignment along the flow direction is obtained by both increasing shear rate and decreasing gap thickness. A critical shear rate was found to be necessary to trigger the alignment. This shear rate occurs in a region where the suspending fluid is only weakly elastic and weakly shear thinning, a result somewhat in contrast with previous literature evidence (Michele et al. 1977; Giesekus 1981).

Alignment along the flow direction is not the only possible flow-induced microstructure. For sufficiently small particles and low shear rates a weak, vorticity-aligned structure was visible by optical microscopy and confirmed by SALS. Such a structure, which has been observed here for the first time, bears analogies with low-shear rate alignment of ellipsoids along the vorticity axis (Johnson and Fuller 1987; Gunes et al. 2008) and may be related to the competition between hydrodynamic and interaction forces. This competition is affected by particle size, but a clear identification of the driving forces is difficult. The present results demonstrate that, depending on the details of the suspending medium and the size and nature of the suspended particles, the formation of aligned structures is affected by the relative magnitude of the colloidal and hydrodynamic forces and the kinetics of string formation versus the kinetics of migration.

Acknowledgements The financial support of Regione Campania (Funds L.5-2007) is gratefully acknowledged. FS thanks FWO-Vlaanderen for a graduate fellowship. JV also acknowledges support of the EU through FP7, project Nanodirect NMP4-SL-2008-213948.

References

Almog Y, Reich S, Levy M (1982) Monodisperse polymeric spheres in the micron size range by a single step process. Br Polym J 14:131–136

Bodvik R, Dedinaite A, Karlson L, Bergstrom M, Baverback P, Pedersen JS, Edwards K, Karlsson G, Varga I, Claesson Per M (2010) Aggregation and network formation of aqueous methylcellulose and hydroxypropylmethylcellulose solutions. Colloids Surf A Physicochem Eng Asp 354:162–171

Brunn P (1976) Slow motion of a sphere in a second-order fluid. Rheol Acta 15:163–171

Giesekus H (1978) Die bewegung von teilchen in stromungen nicht-newtonscher flussigkeiten. Z Angew Math Mech 58: T26–T37

Giesekus H (1981) Some new results in suspension rheology. In: Wendt F (ed) Lect. Ser. 1981–1988, Non-Newt. Flows. Von Karman Inst. for Fl. Dynamics, Rhode Saint Genese

Gunes D, Scirocco R, Mewis J, Vermant J (2008) Effects of aspect ratio and suspending medium rheology on flow-induced orientation of non-spherical particles. J Non-Newton Fluid Mech 155:39–50

Ho BP, Leal LG (1976) Migration of rigid spheres in a two-dimensional unidirectional shear-flow of a second order fluid. J Fluid Mech 76:783–799

Jefri MA, Zahed AH (1989) Elastic and viscous effects on particle migration in plane-Poiseulle flow. J Rheol 33:691–708

Johnson SJ, Fuller GG (1987) The dynamics of colloidal particles suspended in a second-order fluid. Faraday Discuss Chem Soc 83:271–285

Joseph DD, Feng J (1996) A note on forces that move particles in a second order fluid. J Non-Newton Fluid Mech 64: 299–302

Karnis A, Mason SG (1966) Particle motions in sheared suspensions. XIX. Viscoelastic media. Trans Soc Rheol 10: 571–592

Lormand BM, Philips LG (2004) Sphere migration in oscillatory Couette flow of a viscoelastic fluid. J Rheol 48:551–570

Lyon MK, Mead DW, Elliot RE, Leal LG (2001) Structure formation in moderately concentrated viscoelastic suspensions in simple shear flow. J Rheol 45:881–890

Maranzano BJ, Wagner NJ (2002) Flow-small angle neutron scattering measurements of colloidal dispersion microstructures through the shear thickening transition. J Chem Phys 117:10291–10302

Michele J, Patzold R, Donis R (1977) Alignment and aggregation effects in suspensions of spheres in non-Newtonian media. Rheol Acta 16:317–321

Morris JF, Boulay F (1999) Curvilinear flows of noncolloidal suspensions. The role of normal stresses. J Rheol 43:1213–1237

Ponche A, Dupuis D (2005) On instabilities and migration phenomena in cone and plate geometry. J Non-Newton Fluid Mech 127:123–129

Scirocco R, Vermant J, Mewis J (2004) Effect of the viscoelasticity of the suspending fluid on structure formation in suspensions J Non-Newton Fluid Mech 117:183–192

Tehrani MA (1966) An experimental study of particle migration in pipe flow of viscoelastic fluids. J Rheol 40:1057–1077

Won D, Kim C (2004) Alignment and aggregation of spherical particles in viscoelastic fluid under shear flow. J Non-Newton Fluid Mech 117:141–146